Nonlinear Joint-Angle Feedback Control of Electrically Stimulated and λ-Controlled Antagonistic Muscle Pairs

Christian Klauer[1] Jörg Raisch[1,2] Thomas Schauer[1]
[1]Control Systems Group, Technische Universität Berlin, Germany
[2]Systems and Control Theory Group, Max Planck Institute for Dynamics of Complex Technical Systems, Magdeburg, Germany

***Abstract*— In order to control human limb movements in neuro-prosthetic systems, a nonlinear, model-based control strategy for torque generation by antagonistic muscle pairs is presented. The controller based on exact linearization methods enables the tracking of reference joint torque profiles and the generation of pre-defined muscular co-contractions. The controller adjusts the desired recruitment levels λ of both muscles that are controlled by two underlying λ-Controllers automatically compensating muscular fatigue. Estimates on λ are obtained from electrical stimulation evoked Electromyography (EMG)-measurements. Short-term increases of the muscular co-contractions are used to achieve an exact tracking of the accelerating joint torque also in the presence of actuation variable constraints which result from the fact that only positive muscular contractions can occur. The linearization-based controller can serve as underlying controller in cascaded control schemes for the joint-angle or velocity. The feasibility of the proposed approach was demonstrated in a simulation study as well as by a joint-angle control experiment for a healthy subject. Concluding, the authors expect that the proposed approach has a great potential for the future control of artificial limb movements also because of the possibility of modulating the system stiffness by controlled co-contractions of the muscles.**

I. Introduction

Neuro-prosthetic systems aim to induce limb movements by muscular contractions artificially caused by functional electrical stimulation (FES) [8]. Such systems are generally controlled by feedforward or feedback control strategies which modulate the intensity of electrical pulses in terms of charge, current amplitude, pulsewidth or frequency to achieve a certain goal, e.g., tracking a reference trajectory for a joint angle (e.g. [10]).

For joint-angle control, often antagonistic muscle pairs are available for exploitation of actuation, e.g., for the elbow-/knee-joint angle, or for the horizontal shoulder adduction/abduction. The latter will be considered in detail within this contribution. This control problem arises for example in the context of restoring arm function in tetraplegic patients with a high lesion of the spinal cord.

It has been shown that for natural limb movements the involved muscle pairs are not limited to be actuators that solely induce pulling forces into their pre-defined directions. Instead, an important property for the natural control of posture and movement is the ability to allow the modulation of the mechanical impedances due to co-contractions. Naturally, they are modulated by the central nervous system [5].

For FES, more than twenty years ago it was demonstrated, that the involvement of co-contractions can significantly increase the performance of control systems using FES for actuation [3]. The positive effects of co-contractions are already exploited in control of FES (e.g. for compensation of tremor [2], ...).

An important component of muscle modeling and control is the nonlinear, spatial recruitment curve which describes the number of motor units in a muscle activated by FES. This static function, depending on the stimulation intensity, usually includes a threshold at a relative high stimulation level. In order to also control small co-contraction forces, this parameter has to be known exactly for both muscles, otherwise the control system has no information whether the muscle is actually contracted or whether the actuation variable is just acting below the threshold without any influence. Because of muscular fatigue, this parameter is variable in time and hence an on-line identification would be required. However, this is rather difficult when only the summed torque by both muscles is available indirectly through joint-angle measurements.

A promising approach suitable to overcome the problem of inexactly known and time-variant thresholds as well as other muscular properties like fatigue and hysteresis, was presented in an earlier publications [6] and [7]. The aim is to enforce a linear behavior for the nonlinear recruitment curve by feedback (λ-Control) of an estimate of the muscular recruitment λ (amount of activated motor neurons). The stimulation intensity is adjusted such that a reference recruitment level r_λ is tracked. Controllers for neuro-prosthetic systems would then use this reference for the muscular recruitment instead of the stimulation intensity as their actuation variable(s).

In this work, a strategy for modulation of a desired accelerating torque along with a co-contraction torque in form of a linearizing controller is presented. This controller acts on top of two λ-Control loops for each muscle respectively. The linearizing controller is based on system inversion for time discrete systems. Since the signals for the actuation of each muscle are constraint to be positive, an extension of the linearizing controller is investigated that guarantees exact inversion with regard to the accelerating torque at the cost of a temporally increased co-contraction torque. For demonstrating this concept, a linear joint-angle controller acting on top of the linearizing controller is designed.

Sec. II describes the experimental set-up. A model for control design is introduced in Sec. III followed by the linearization controller in Sec. IV. In Sec. V a linear feedback controller for controlling the joint angle is designed for demon-

strating the usefulness of the underlying linearizing controller. Results are presented in Sec. VI and final conclusions are given in Sec. VII.

II. Control scheme & experimental set-up

A. Experimental set-up

The used set-up is shown in Fig. 1 and consists of an passive exoskeleton (ARMEO, Hocoma AG, Switzerland) for weight compensation with angle sensors, a stimulation system (REHASTIM, Hasomed GmbH, Germany), a 24-bit EMG-amplifier (PHYSIOSENSE, developed at TU Berlin), an inertial motion unit (IMU) (RAZORIMU 9DOF, Sparkfun, United Kingdom) and a PC running Linux with RT-Preemption-Patch. All devices are connected to the PC through USB interfaces.

The subject's arm is placed inside the exoskeleton as shown and the arm movement is limited to horizontal shoulder abduction and adduction. The corresponding angle ϑ is defined as shown in Fig. 1 whereas $\vartheta = 0$ describes the rest position of the arm. This angle and its first time derivative are determined by fusing the outputs of the exoskeleton angle sensors and the IMU information.

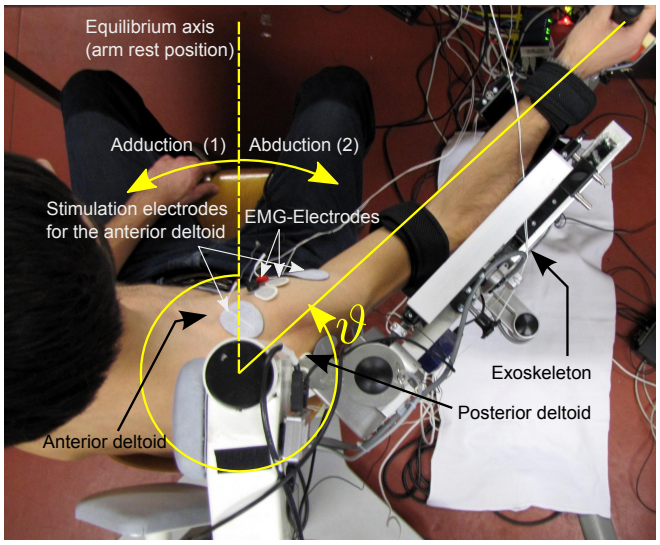

Fig. 1 - Experimental Set-up.

Current-controlled stimulation impulses are applied through self-adhesive hyrdo-gel electrodes at a stimulation frequency of 28 Hz. The anterior part of the deltoid muscle is stimulated to cause horizontal shoulder adduction. Horizontal abduction is produced by stimulation of the posterior part of the deltoid muscle. Signals related to adduction and abduction will be denoted by the indices 1 and 2 respectively. For EMG measurement at the stimulated muscles, smaller AgCl electrodes are placed between each pair of stimulations electrodes. The FES evoked EMG (eEMG) is recorded at a sampling rate of 4kHz.

For both muscles, the eEMG is filtered as described in [6] to estimate the states $\lambda_i, \quad i = 1,2$, of muscle recruitment. Two λ-controllers, also introduced in [6], automatically adjust the stimulation intensity (pulse charge) in order to generate the desired recruitment levels $r_{\lambda_i}, \quad i = 1,2$.

The open source real-time dynamic block simulation system OPENRTDYNAMICS (http://openrtdynamics.sf.net) is used for implementation of all time critical components and provides a network communication to a QT4-GUI. The design of the control system is carried out with help of the program system SCILAB (http://www.scilab.org).

III. Neuro-Musculoskeletal Model

To describe the joint angle dynamics with FES actuation, a Hill-type muscle model [4] succeeded by a second order mechanical system is assumed. This model along with methods for parameter estimation is described in [11].

A. Muscle model including λ-Controller

The muscular model part, which also includes the closed loop of the λ-Controller as shown in Fig. 2, describes the generated torque T_i for each muscle i respectively. Because the muscles are λ-controlled, the inputs are the references for the recruitment levels.

Internally, the λ-Control systems adjust the stimulation intensities v_i for each muscle i such that the muscular recruitment levels λ_i follow their references r_{λ_i}. Hereby, integral controllers are used to control the one step delayed output of the recruitment functions rc_i (the estimated muscular recruitment $\hat{\lambda}$). These functions commonly consist of a threshold, a saturation and an approximatively linear behavior inbetween. For the ongoing control design, the resulting closed loop systems are assumed to be linear, whereby the reference to output behaviors are then described by the transfer functions T_{λ_i}. Each λ-Controller gain is determined by obtaining a linear model of rc_i and a subsequent pole placement design as described in [6]. The ability to compensate for muscular fatigue and time variant thresholds in rc_i was shown in [7].

The calcium dynamics G_m models the dependency of the muscle activation σ_i on λ_i. The recruitment λ_i, its reference r_{λ_i}, the stimulation intensity v_i as well as the muscular activation σ_i are constrained to be non-negative. The calcium dynamics can be approximated by a continuous-time transfer function of first order without zeros and a time delay T_{md}. The transfer function is time discretized using Euler discretization:

$$G_m^*(q^{-1}) = 1/(sT_{ca}+1)|_{s=(1-q^{-1})/T_a}.$$

Here, q^{-1} is the backward shift operator and $T_a = 36\,\text{ms}$ is the sampling period. The approximative time constant $T_{ca} = 0.04\,\text{s}$ is chosen with reference to [9]. The time delay of the calcium dynamics is approximated by a delay of two sampling steps (q^{-2}), which matches to measured data quite well. The closed loop systems T_{λ_i} are discrete-time first order system without dead time and zeros [6].

Finally, the muscular torque T_i is then modeled by the multiplication of a function f_i with σ_i. The function f_i linearly depends on the joint angle and is modeled by:

$$f_i(k) = k_{s,i}(\vartheta_{max,i} - \vartheta(k)).$$

The parameters $\vartheta_{max,i}$ represent the boundaries of the operational angular space $\vartheta \in [\vartheta_{max,2}, \vartheta_{max,1}]$ and describe

reachable joint angles. The gains $k_{s,1}$ and $k_{s,2}$ are strictly positive, which results in $f_1 \geq 0$ and $f_2 \leq 0$ and further in $T_1 \geq 0$ and $T_2 \leq 0$ respectively because of $\sigma_i \geq 0$.

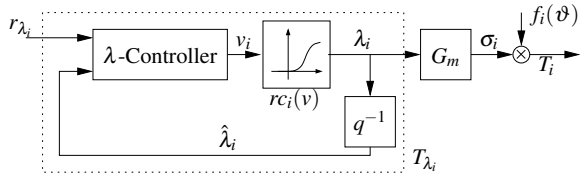

Fig. 2 - The model for one λ-Controlled muscle path. Given a reference r_{λ_i} for the muscular recruitment λ_i, the controller adjusts the stimulation intensity v_i. The nonlinear recruitment function rc_i describes the recruitment. The resulting closed loop T_{λ_i} has an approximatively linear dynamics. The calcium dynamics G_m models the dependency of the muscular activation σ_i on λ_i. The muscular torque T_i is then modeled by the multiplication of the angle-dependent function f_i with σ_i.

For the linearizing controller designed later on, the slightly more conservative constraints $f_1 > 0$ and $f_2 < 0$ must be applied. Therefore, the valid range for the joint angle is reduced to $\vartheta \in]\vartheta_{max,2}, \vartheta_{max,1}[$.

The total muscle model is then described by

$$T_i(k) = \underbrace{k_{s,i}(\vartheta_{max,i} - \vartheta(k))}_{f_i(k)} \cdot \underbrace{\frac{q^{-2}(1-a)}{1-aq^{-1}}}_{q^{-2}G_m^*(q^{-1})} \cdot \underbrace{\frac{1-b_i}{1-b_iq^{-1}}}_{T_{\lambda_i}(q^{-1})} r_{\lambda_i} \quad (1)$$

where k is the sampling index. The parameters $a \in [0,1[$ and $b_i \in [0,1[$ lead to an asymptotically stable system.

B. Resulting acceleration and co-contraction torque

For describing a torque T which leads to an acceleration of the mechanical system (arm) and to a co-contractive torque T_{cc}, which describes the amount of co-contracting torques in an antagonistic muscle pair, a transformation between both muscular induced torques T_i and the resulting torques T and T_{cc} is introduced.

The accelerating torque T is given by the operation

$$\mathcal{T}(T_1, T_2) := T_1 + T_2, \qquad T_1 \geq 0,\ T_2 \leq 0. \quad (2)$$

The co-contraction torque $T_{cc} \geq 0$ is obtained by the following operator:

$$\mathcal{T}_{cc}(T_1, T_2) := \min(T_1, -T_2) \quad (3)$$

The inverse transformation operator $\mathcal{T}_1^I$ is then

$$\mathcal{T}_1^I(T_{cc}, T) := \begin{cases} T_{cc} + T & T \geq 0 \\ T_{cc} & T < 0 \end{cases}, \quad (4)$$

and analog

$$\mathcal{T}_2^I(T_{cc}, T) := \begin{cases} -T_{cc} & T \geq 0 \\ -T_{cc} + T & T < 0 \end{cases}. \quad (5)$$

The torques T and T_{cc} are then described by

$$\begin{aligned} T(k) &= \mathcal{T}(T_1(k), T_2(k)), \\ T_{cc}(k) &= \mathcal{T}_{cc}(T_1(k), T_2(k)). \end{aligned}$$

C. Mechanical model

The input to the mechanical model are the resulting torques T and T_{cc}. Because of the one dimensional movement, a second order system including a viscous friction R_m and the elasticity K_m is used. The differential equation in terms of the joint angle ϑ is

$$\ddot{\vartheta} = \frac{1}{J}\left[T - R_m(T_{cc})\dot{\vartheta} - K_m(T_{cc})\vartheta\right] \quad (6)$$

A modulation of the mechanical impedance by the co-contraction torque T_{cc} is assumed. In this case, the parameters for the viscous friction R_m and the elasticity K_m depend on T_{cc}. The design of a model for these functions would go beyond the scope of this paper and forms future research topics. Therefore, for controller design this modulation of the system properties is neglected and only the constants obtained through system identification for zero co-contraction are used.

The complete model including the λ-controlled muscles and the mechanical system is presented in Fig. 3. The mechanical model as described in [11], also accounts for a static friction term, which is neglected in this work.

IV. Linearizing Controller

The multiplication inside the muscle models with the internal feedback signal f_i leads to a non-linear system behavior. Since the mechanical system is already linear, only the muscular part, which contains the multiplication, is linearized. Therefore, a state space representation of (1) is derived with $\overline{\lambda}_i = q^{-1}\lambda_i$:

$$\begin{aligned} \overline{\lambda}_i(k+1) &= b_i\overline{\lambda}(k) + (1-b_i)r_{\lambda,i} & (7) \\ \sigma_i(k+1) &= a\sigma_i(k) + (1-a_i)\overline{\lambda}_i(k) & (8) \\ T_i(k) &= \sigma_i(k)f_i(k). & (9) \end{aligned}$$

For describing the muscular torque induced by each muscle i with two time steps delay, two functions $\mathcal{T}_i, i = 1,2$, are introduced that depend on the actuation variables $r_{\lambda_i}(k)$:

$$\begin{aligned} \mathcal{T}_i(r_{\lambda_i}) \quad := \quad & f_i(k+2)\left[a\sigma_i(k+1) + \right. \quad (10) \\ & \left. +(1-a_i)\left[b_i\lambda_i(k) + (1-b_i)r_{\lambda_i}\right]\right] \end{aligned}$$

The modeled torque is then described by $T_i(k+2) = \mathcal{T}_i(r_{\lambda_i}(k))$. For the control law, two functions

$$\begin{aligned} \mathcal{R}_{\lambda_i}(u_i) \quad := \quad & \frac{1}{1-b_i}\left[-b_i\lambda_i(k) + \right. \\ & \left. +\frac{1}{1-a_i}\left[-a\sigma_i(k+1) + \frac{1}{f_i(k)}u_i\right]\right] \quad (11) \end{aligned}$$

are introduced with $i = 1,2$. By assigning them to the actuation variables $r_{\lambda_i} = \mathcal{R}_{\lambda_i}(u_i(k))$ the system (1) is exactly linearized. Eq. (11) depends on the future internal mechanical feedback variable $f_i(k+2)$ as well as on the state variables $\sigma_i(k+1)$ and $\lambda_i(k)$. The states are calculated by two internal models implementing (7) and (8) for $i \in 1,2$, whereby the actuation variables $r_{\lambda_i}(k)$ are applied to this internal system. An estimation of $f_i(k+2)$ is used instead of the real signal, that is calculated by a two-step ahead prediction (see

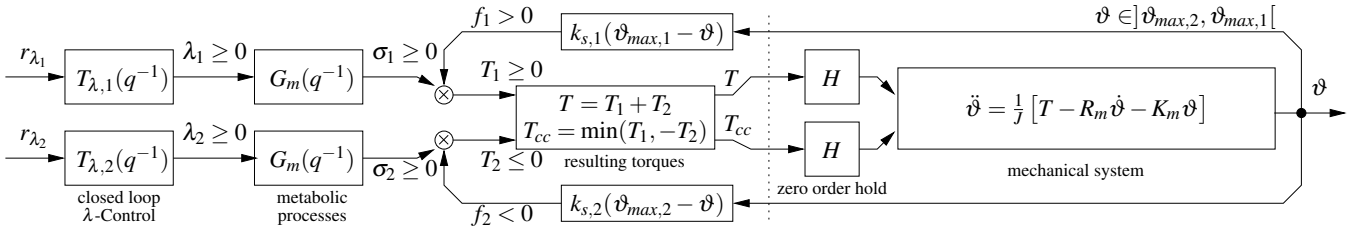

Fig. 3 - Neuro-musculoskeletal model used for controller design.

paragraph *Two step ahead joint-angle prediction*) of the joint angle.

By applying the linearizing controllers to Eq. (10), the virtual plants

$$T_i(k+2) = u_i(k),\, i = 1,2$$

result. Each forms a delay of two sampling steps.

For outer control loops it is preferable to formulate the desired torques in terms of resulting torques $T_d = \mathcal{T}(T_{1,d}, T_{2,d})$ and $T_{cc,d} = \mathcal{T}_{cc}(T_{1,d}, T_{2,d})$. The inverse transformations $\mathcal{T}_i$ are used to calculate $T_{i,d}$. In a case, where no constraints for the actuation variables are considered, $T_{i,d}$ are directly applied to the virtual inputs u_i of the linearization controller:

$$u_i(k) = T_{i,d}(k). \tag{12}$$

Again, by applying the linearizing controller to both muscles we obtain the resulting torques

$$T_{cc}(k+2) = T_{cc,d}(k), \qquad T(k+2) = T_d(k).$$

In practice, exact linearization in this form cannot always be achieved because the actuation variables must fulfill $r_{\lambda_1}(k) \geq 0 \wedge r_{\lambda_2}(k) \geq 0$.

A. Constrained actuation variables

Since both actuation variables are actually constrained by $r_{\lambda_i}(k) \geq 0$ for $i = 1,2$, a possible improvement of linearization in case of violated constraints is investigated. For this analysis, different cases are considered:

CASE 1: $\mathcal{R}_{\lambda_1,k}(T_{1,d}) \geq 0 \wedge \mathcal{R}_{\lambda_2,k}(T_{2,d}) < 0$
CASE 2: $\mathcal{R}_{\lambda_1,k}(T_{1,d}) < 0 \wedge \mathcal{R}_{\lambda_2,k}(T_{2,d}) \geq 0$
CASE 3: $\mathcal{R}_{\lambda_1,k}(T_{1,d}) < 0 \wedge \mathcal{R}_{\lambda_2,k}(T_{2,d}) < 0$.

For each case, different extensions to the linearizing controller are analyzed. By considering both paths at the same time, the behavior of the resulting accelerating torque T depending on the desired inputs T_d can be linearized, this time including the constraints. As it turns out in the analysis, this usually leads to the drawback of an increased co-contraction torque T_{cc} compared to the desired one $T_{cc,d}$.

Fig. 4 shows the linearizing controller along with the nominal model including the constraints on the actuation variables $r_{\lambda_i}(k)$. Unlike equation (12), additionally an extension is added, which feeds additive correction terms $u_{i,a}$ to the actuation variables u_i such that $T = T_d$ can be achieved:

$$u_1(k) = T_{1,d}(k) + u_{1,a}(k), \qquad u_2(k) = T_{2,d}(k) + u_{a,2}(k). \tag{13}$$

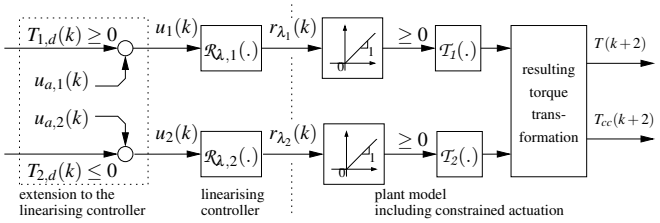

Fig. 4 - An extension is applied to the linearizing controller in the presence of constrained actuation by modification of the signals u_1 and u_2. The calculated actuation variable of the linearization controller is applied to the plant, which additionally includes the constraints on the actuation variables $r_{\lambda_i}(k)$.

Because of the dynamics of the muscle contraction and the λ-Control loop, the muscular activations $\sigma_i(k+1)$ are not necessarily zero for zero actuation. Instead, the smallest muscular activation possible is achieved by choosing $r_{\lambda_i}(k) = 0$ as negative actuation variables are not possible. The torques produced by each muscle in this case are called minimum torques:

$$T_{1,min} := \mathcal{T}_1(0) = f_1(k+2)(a\sigma_1(k+1) + (1-a)b_1\lambda_1(k)) \geq 0,$$
$$T_{2,min} := \mathcal{T}_2(0) = f_2(k+2)(a\sigma_2(k+1) + (1-a)b_2\lambda_2(k)) \leq 0.$$

At first, monotonic properties of $\mathcal{R}_{\lambda_i}$ (Eq. (11)) have been investigated. Therefore, the control law is rearranged:

$$\mathcal{R}_{\lambda_i}(u_i(k)) := \underbrace{-\frac{1}{1-b_i}\left[b_i\lambda_i(k) + \frac{1}{1-a}a\sigma_i(k+1)\right]}_{>0} + \underbrace{\frac{1}{1-b_i}\frac{1}{1-a}}_{>0}\frac{1}{f_i(k+2)}u_i(k).$$

Because of $f_1 > 0$, $\mathcal{R}_{\lambda_1}(u_1)$ is strictly monotonically increasing ($\mathcal{R}_{\lambda_1}(u_1^l) < \mathcal{R}_{\lambda_1}(u_1^h)$, for $u_1^l < u_1^h$) and $\mathcal{R}_{\lambda_2}(u_2)$ monotonically decreasing, since $f_2 < 0$.

Similar results are obtained for the functions $\mathcal{T}_1$ (strictly monotonically increasing) and $\mathcal{T}_2$ (strictly monotonically decreasing) with respect to the arguments r_{λ_1} and r_{λ_2} respectively.

a) CASE 1*:* $\mathcal{R}_{\lambda_1}(T_{1,d}) \geq 0 \wedge \mathcal{R}_{\lambda_2}(T_{2,d}) < 0$

The calculated actuation variable r_{λ_2} would be negative and would be be set to zero. Therefore, the requested torque for the second path $i = 2$ (always negative torques for this path) is bigger than the actually achievable torque $T_{2,min}$:

$$T_{2,min}(k+2) = \mathcal{T}_2(0) < \mathcal{T}_2(\mathcal{R}_{\lambda_2}(T_{2,d}(k))) = T_{2,d}(k). \tag{14}$$

This is because $\mathcal{R}_{\lambda_2}(T_{2,d}) < 0$ and $\mathcal{T}_2$ is monotonically decreasing. With active constraints and without additional measures ($u_{a,i} = 0, i = 1,2$) the resulting acceleration torque is smaller than the requested one T_d:

$$\mathcal{T}_1(\mathcal{R}_{\lambda,1}(T_{1,d}(k))) + T_{2,min}(k+2) < T_d(k), \tag{15}$$

By choosing the modified actuation variable $u_1 = T_{1,d} + u_{a,1}$ the requirement on the resulting torque can be achieved if

$$\begin{aligned} \mathcal{T}_1(\mathcal{R}_{\lambda,1}(\underbrace{T_{1,d}(k) + u_{a,1}(k)}_{u_1(k)})) + T_{2,min}((k+2) = \quad & T_d(k) \quad (16) \\ T_{1,d}(k) + u_{a,1}(k) + T_{2,min}(k+2) = \quad & T_d(k) \end{aligned}$$

is true.

Using (15) and (16) it can be shown that $u_{a,1} > 0$ and further $\mathcal{R}_{\lambda,1}(T_{1,d} + u_{a,1}) > 0$ holds, because $T_{1,d} > 0$.

Now, eq. (16) is solved with respect to $u_{a,1}$:

$$u_{a,1}(k) = T_d(k) - T_{2,min}(k+2) - T_{1,d}(k). \tag{17}$$

The variables u_i that fulfill the constraints for r_{λ_i} and yield $T(k+2) = T_d(k)$ are then

$$u_1(k) = T_d(k) - T_{2,min}(k+2), \quad u_2(k) = T_{2,min}(k+2).$$

The corresponding activation variables are then

$$r_{\lambda_1}(k) = \mathcal{R}_{\lambda,1}(T_d(k) - T_{2,min}(k+2)), \quad r_{\lambda_2}(k) = 0.$$

b) CASE 2*:* $\mathcal{R}_{\lambda_1}(T_{1,d}) < 0 \wedge \mathcal{R}_{\lambda_2}(T_{2,d}) \geq 0$

Because of symmetry reasons, the procedure is analog to CASE 1. Here, the achieved torque for the muscle path 1 would be greater than the desired one (as the corresponding muscle can not be deactivated fast enough). Therefore, the variable u_2 of the antagonistic path has to be decreased by choosing:

$$u_{a,2}(k) = T_d(k) - T_{1,min}(k+2) - T_{2,d}(k). \tag{18}$$

The variables u_i that fulfill the constraints for r_{λ_i} and yield $T(k+2) = T_d(k)$ are then

$$u_1(k) = T_{1,min}(k+2), \quad u_2(k) = T_d(k) - T_{1,min}(k+2).$$

The corresponding activation variables are then

$$r_{\lambda_1}(k) = 0, \quad r_{\lambda_2}(k) = \mathcal{R}_{\lambda,2}(T_d(k) - T_{1,min}(k+2)).$$

c) CASE 3*:* $\mathcal{R}_{\lambda_1,k}(T_{1,d}) < 0 \wedge \mathcal{R}_{\lambda_2,k}(T_{2,d}) < 0$

Because both constraints for the actuation variables are violated within CASE 4, the resulting accelerating torque would be $T_{1,min} + T_{2,min}$, which is not necessarily equal to the desired torque T_d. For determination of the compensation variables $u_{a,1}$ and $u_{a,2}$, two sub-cases are considered:

4.1) $T_d > T_{1,min} + T_{2,min}$ (actual torque too small)
4.2) $T_d < T_{1,min} + T_{2,min}$ (actual torque too big)

At first CASE 4.1) is evaluated. In order to achieve the desired accelerating torque T_d, the torque T_1 needs to be increased. This can be fulfilled by applying the additional desired torque $u_{1,a}$ such that

$$T_d(k) = \mathcal{T}_1(\mathcal{R}_{\lambda_1}(T_{1,d}(k) + u_{1,a}(k))) + T_{2,min}(k+2). \tag{19}$$

Because of (19) and the condition for CASE 4.1,

$$\mathcal{T}_1(\mathcal{R}_{\lambda_1}(T_{1,d}(k) + u_{1,a}(k))) \geq T_{1,min}(k+2) \geq 0$$

holds. Further, because $\mathcal{T}_1$ is monotonically increasing, also $\mathcal{R}_{\lambda_1}(T_{1,d} + u_{1,a}) \geq 0$ must hold, which means the constraint for the first actuation variable is satisfied. In this case, Eq. (19) becomes:

$$T_d(k) = T_{1,d}(k) + u_{1,a}(k) + T_{2,min}(k+2).$$

By rearranging, $u_{1,a}$ can be calculated leading to

$$u_{1,a}(k) = T_d(k) - T_{1,d}(k) - T_{2,min}(k+2).$$

The variables u_i that fulfill the constraints for r_{λ_i} and yield $T(k+2) = T_d(k)$ are then

$$u_1(k) = T_d(k) - T_{2,min}(k+2), \quad u_2(k) = T_{2,min}(k+2).$$

The corresponding activation variables are then

$$r_{\lambda_1}(k) = \mathcal{R}_{\lambda,1}(T_d(k) - T_{2,min}(k+2)), \quad r_{\lambda_2}(k) = 0.$$

For CASE 4.2) an analog procedure leads to following result. The variables u_i that fulfill the constraints for r_{λ_i} and yield $T(k+2) = T_d(k)$ are then

$$u_1(k) = T_{1,min}(k+2), \quad u_2(k) = T_d(k) - T_{1,min}(k+2).$$

The corresponding activation variables are

$$r_{\lambda_1}(k) = 0, \quad r_{\lambda_2}(k) = \mathcal{R}_{\lambda,2}(T_d(k) - T_{1,min}(k+2)).$$

For all three cases it is straightforward to show that exact tracking of T_d can only be achieved by inducing a co-contraction of the two muscles.

B. Two step ahead joint-angle prediction

The mechanical system (6) is time discretized:

$$\begin{aligned} x_1(k+1) = \quad & x_1(k) + T_a[x_2(k)] & (20) \\ x_2(k+1) = \quad & x_2(k) + \tfrac{T_a}{J}[-R_m x_2(k) - K_m x_1(k) + T(k)]. & (21) \end{aligned}$$

By substituting $k \to k+1$ in Eq. (20), replacing $x_2(k+1)$ by Eq. (21) and further replacing $x_1(k+1)$ by the right hand side of Eq. (20) a two step ahead prediction for the joint angle is derived:

$$\begin{aligned} \hat{x}_1(k+2) \quad = \quad & x_1(k) + T_a x_2(k) + T_a \Big[x_2(k) + \quad (22) \\ & + \frac{T_a}{J}\left[-R_m x_2(k) - K_m x_1(k) + T(k)\right] \Big]. \end{aligned}$$

The accelerating torque $T(k)$ is replaced by the desired one $T_d(k-2)$, since $T(k)$ can not be measured and $T(k) = T_d(k-2)$ as enforced by the linearizing controller in the nominal case. The state variables x_1 and x_2, which refer to the joint angle ϑ and its derivation in time $\dot{\vartheta}$ are measured.

Now, the estimates of $f_i(k+2), i = 1,2$, are determined by

$$\hat{f}_i(k+2) = k_{s,i}(\vartheta_{max,i} - \hat{\vartheta}(k+2)). \tag{23}$$

TABLE I

TABLE OF PARAMETERS

(a)

simulation parameters	
Parameter	Value
K_m/J	$4.015[\mathrm{s}^{-2}]$
R_m/J	$1.28[\mathrm{s}^{-1}]$
$\vartheta_{max,1}$	0.52[rad]
$\vartheta_{max,2}$	-1.57[rad]
$k_{s,1}/J$	$4.84[\mathrm{s}^{-2}]$
$k_{s,2}/J$	$2.357[\mathrm{s}^{-2}]$
a	0.678
b_1	0.811
b_2	0.845

(b)

real parameters	
Index	Value
K_m/J	$4.42[\mathrm{s}^{-2}]$
R_m/J	$2.82[\mathrm{s}^{-1}]$
$\vartheta_{max,1}$	1.047[rad]
$\vartheta_{max,2}$	-2.61[rad]
$k_{s,1}/J$	$1.188[\mathrm{s}^{-2}]$
$k_{s,2}/J$	$0.846[\mathrm{s}^{-2}]$
a	0.678
$b_1 = b_2$	0.65
controller parameters	
d	0.5
T_r	$0.3[s]$
s_1	-3
s_2	-4

V. LINEAR JOINT-ANGLE FEEDBACK CONTROL

On top of the linearizing controller, a linear, time-discrete and two degree of freedom joint angle controller is applied that uses the desired torque T_d as its actuation variable. The mechanical model Eq. (6) is Euler discretized and used as transfer function for controller design:

$$G(z) = \frac{T_a^2/J}{z^2 + (\frac{R_m T_a}{J} - 2)z + (K_m T_a^2 - T_a R_m + 1)/J}.$$

The time delay of the system is neglected since it is considerable low compared to the rise time of G. The controller K cancels the asymptotically stable plant G and introduces a new second order transfer function to the open loop:

$$K(z) = 1/G(z)\frac{a_0}{z^2 + b_1 z + b_0}.$$

The transfer function

$$G_{cl}(z) = \frac{a_0}{z^2 + b_1 z + b_0 + a_0} \tag{24}$$

describes the reference to output behavior and is considered for the specification of the closed-loop behavior (assuming at first no pre-filter for the reference).

The parameters a_0, b_0 and b_1 are determined by a pole-placement procedure for the denumerator of G_{cl} and by claiming unity gain for G_{cl} ($G_{cl}(z=1)=1$). The latter condition leads to an integral controller. A desired second order pole pair [1] described by a damping d and a rise time T_r is used for the pole -placement design.

Additionally to the feedback controller K, a reference pre-filter V is designed to cancel the reference to output behavior G_{cl} and to introduce a slower second order dynamical system without conjugate complex poles:

$$V(z) = 1/G_{cl}(z) \cdot \frac{(1-\exp(-s_1 T_A)\cdot(1-\exp(-s_2 T_A)}{(z-\exp(-s_1 T_A)\cdot(z-\exp(-s_2 T_A)}.$$

VI. RESULTS

For demonstrating the effectiveness of the linearizing controller along with its extension for the given constraints, a comparison of the controller with and without the extension was performed in form of a simulation study. Predefined trajectories were fed to the desired torques T_d and $T_{d,cc}$, while the torques of the plant model (cf. sec. III.) were evaluated. For the model and the linearizing controller the parameters described in Tab. I(a) were used. In the Figs. 6 and 5 the results in form of a comparison of the desired torques (T_d, $T_{cc,d}$) and the actual torques (T, T_{cc}) are presented. Additionally, the actuation variables are shown.

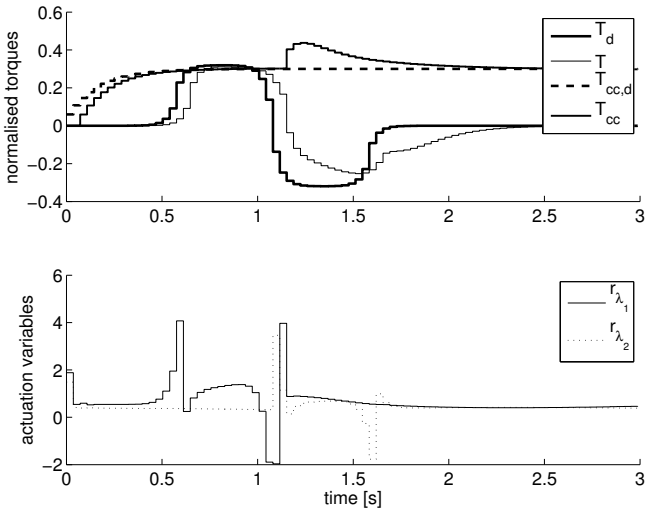

Fig. 5 - Results for the linearization controller without taking constraints on the actuation variables into account. The actuation variables shown in the lower subplot also show the computed negative values. However, for the simulated model the constraints $r_{\lambda,i} \geq 0$ were applied. Thus, values violating these constraints were set to zero.

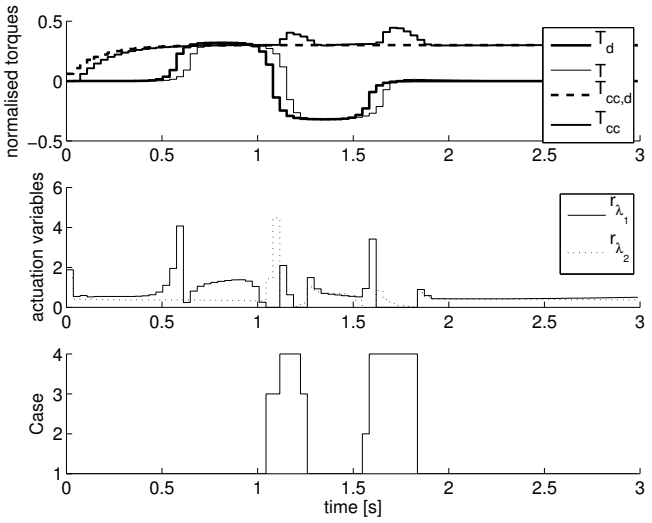

Fig. 6 - Results for the extended linearization controller.

For the linearizing controller without the extension, there is a considerable mismatch of T compared to the reference

T_d. For an upper level joint-angle controller this would lead to a decrease of the achievable performance. However, when the extension is enabled, T_d is matched (just leading to a time delay of two sampling steps). Small derivations (not visible in the plot) are due to the time-discretized plant model within the joint-angle prediction (cf. Sec. IV-B).

The feasibility of the developed approach is further demonstrated by a joint-angle control experiment for one healthy subject. Before the control experiment, the λ-Control loops were tuned and the model (cf sec. III.) was identified using the procedure described in [11]. The resulting parameters are summarized in Tab. I(b). The results for the control experiment for a stepwise changing reference are shown in Fig. 7. The desired co-contraction torque $T_{cc,d}$ was zero since also no co-contraction was present in the experiment for parameter identification. The resulting co-contraction torque was of course temporally greater than zero to fulfill $T = T_d$ when violating actuation variable constraints. Additionally to the measured joint angle ϑ, the nominal behavior ϑ_{nom} (if the joint angle controller is applied to the linear plant model G) is shown. As the step size increases, the overshoot of the joint angle increases as under an increasing distance of ϑ to its equilibrium, the validity of the assumed model decreases.

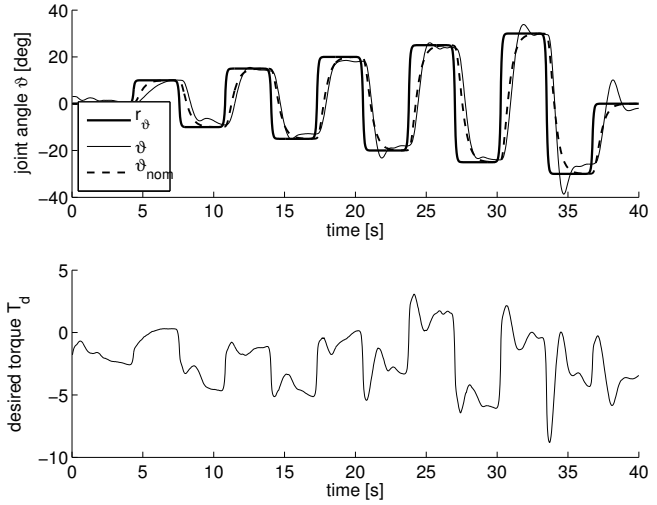

Fig. 7 - Results of a joint-angle control experiment for a healthy subject using the underlying linearization controller with extension and two λ-Control loops. The desired co-contraction torque $T_{cc,d}$ was zero.

VII. Conclusions and Outlook

The presented control strategy for antagonistic muscle pairs allows the control of accelerating torques along with the possibility to modulate the co-contraction strength. In a simulation study the effectiveness of the proposed model inversion that takes actuation constraints into account was shown.

The entire control system, including the linearization and the upper level joint-angle controller, was successfully tested on one healthy subject. Closeness of ϑ and ϑ_{nom} shows the suitability of the proposed approach.

Using two underlying λ-Controllers for each muscle respectively, the inner control system rapidly compensates for fatigue and changing muscular thresholds, which is a prerequisite for the practical application of neuro-prosthetic systems in clinical environments.

Further investigation of the influence of co-contractions on the mechanical stiffness and elasticity is ongoing. In this field, the authors expect a great potential for the artificial control of limb movements.

Acknowledgment

The research leading to these results has received funding from the European Community's Seventh Framework Programme under grant agreement no. 248326 within the project MUNDUS.

References

[1] K. J. Åström and B. Wittenmark. *Computer-Controlled Systems: Theory and Design*. Prentice Hall, 1997.

[2] A.P.L. Bó and and P. Poignet. Tremor attenuation using FES-based joint stiffness control. In *Robotics and Automation (ICRA), 2010 IEEE International Conference on*, pages 2928–2933, may 2010.

[3] W.K. Durfee. Task-based methods for evaluating electrically stimulated antagonist muscle controllers. *Biomedical Engineering, IEEE Transactions on*, 36(3):309–321, march 1989.

[4] A. V Hill. *First and last experiments in muscle mechanics*. Cambridge UP, 1970.

[5] N Hogan. Adaptive control of mechanical impedance by coactivation of antagonist muscles. *IEEE Transactions on Automatic Control*, 29(8):681–690, 1984.

[6] C. Klauer, J. Raisch, and T. Schauer. Linearisation of electrically stimulated muscles by feedback control of the muscular recruitment measured by evoked EMG . In *Proc. of MMAR 2012*, page 108–113, Miedzyzdroje, Poland, 2012. IEEE.

[7] C. Klauer, J. Raisch, and T. Schauer. Advanced Control Strategies for Neuro-Prosthetic Systems. In *Proc. of TAR 2013*, Berlin, Germany, 2013.

[8] P Hunter Peckham and Jayme S Knutson. Functional electrical stimulation for neuromuscular applications. *Annual Review of Biomedical Engineering*, 7:327–360, 2005.

[9] R. Riener and T. Fuhr. Patient-driven control of FES-supported standing up. *IEEE Trans. Rehabil. Eng*, 6(2):113–124, 1998.

[10] Riener Robert. Model–based Development of Neuroprostheses for Paraplegic Patients. *Philosophical Transactions of the Royal Society of London. Series B: Biological Sciences*, 354(1385):877–894, May 1999.

[11] P. Spagnol, C. Klauer, F. Previdi, J. Raisch, and T. Schauer. Modeling and Online-Identification of Electrically Stimulated Antagonistic Muscles for Horizontal Shoulder Abduction and Adduction. In *Proc. of ECC 2013*, Zürich, Switzerland, 2013.